

Heterogeneous, Defect-Rich Battery Particles and Electrodes: Why Do They Matter, and How Can One Leverage Them?

Zhijie Yang and Feng Lin*



Cite This: *J. Phys. Chem. C* 2021, 125, 9618–9629



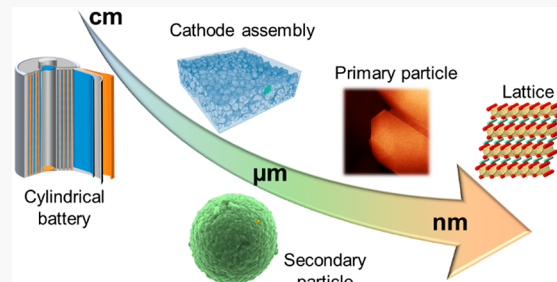
Read Online

ACCESS |

Metrics & More

Article Recommendations

ABSTRACT: Correlating local materials properties with global battery electrochemistry is nontrivial, because battery particles and electrodes are heterogeneous and defect-rich. Pinpointing the root cause of battery performance improvement or degradation can be challenging. Herein, we discuss our recent progress in understanding electrode heterogeneities and structural defects in Li ion and Na ion cathodes ranging from individual particles to electrode ensembles, with a focus on leveraging spectroscopic imaging techniques. Based on our recent studies, this Perspective attempts to shed light on these questions: How heterogeneous are the electrochemical reactions within and among active particles? What are the roles of structural defects (point defects, dislocations, grain boundaries, cracks) in directing electrochemical reactions? Are analytical techniques capable of characterizing these heterogeneities with good statistical representativeness? How will the characterization results inform better design of chemical heterogeneity, such as engineered dopant distribution, to improve battery performance? Can we tailor structural defects to improve battery performance? Given the prevailing heterogeneities reported in our studies and others', we also discuss potential pitfalls of high-resolution data interpretation and highlight the significance of combining characterizations at different length scales and using advanced data analytics to improve result robustness.



1. INTRODUCTION

Rechargeable Li ion batteries have extensively permeated every aspect of daily lives, with applications focusing on consumer electronics and electric vehicles. In 1991, the Sony Corporation first commercialized Li ion batteries, which adopted LiCoO_2 as the cathode and graphite as the anode.¹ Over the last decades, the battery community has made great efforts in developing high-energy cathode materials to meet the increasing energy need. Meanwhile, enhancement of the energy utilization efficiency of individual battery particles is equally significant regardless of the types of cathode materials. A typical cathode architecture contains cathode active materials, conductive additives, and binder. To extensively exploit the energy of the cathode, each of the active electrode particles should fully contribute to the capacity. However, do all active material particles deliver the capacity completely and simultaneously? In other words, are electrochemical reactions homogeneous within and among active particles? If not, how heterogeneous are the electrochemical reactions within and among active particles? What are the roles of structural defects (point defects, dislocations, grain boundaries, cracks) in directing electrochemical reactions? Are analytical techniques capable of characterizing these heterogeneities with good statistical representativeness? How will the characterization results inform better design of chemical heterogeneity, such as engineered dopant distribution, to improve battery performance?

ance? Can we tailor structural defects to improve battery performance?

Recent studies have recognized a large extent of state of charge (SOC) heterogeneity in the state-of-the-art layered cathode materials, which can induce undesired capacity loss, local overcharge/discharge, etc.^{2,3} For example, Xu et al. investigated SOC distribution in individual LiCoO_2 cathode particles upon electrochemical cycling.² When charged to 4.6 V at the current rate of 1C ($n\text{C}$ represents a full charge or discharge of the electrode in $1/n$ hour), ~82% of the LiCoO_2 particle was at the charged state. After the subsequent discharging to 3 V at 1C, only ~50% of the LiCoO_2 particle reverted to the discharged state, which suggested a highly heterogeneous, asymmetric reaction process and inefficient utilization of active particles upon battery cycling.² Furthermore, the SOC heterogeneity also widely exists in olivine (e.g., LiFePO_4) and spinel (LiMn_2O_4) cathode materials.^{4–6} For example, Lim et al. monitored the Li dynamics and phase

Received: February 25, 2021

Revised: April 14, 2021

Published: April 28, 2021



ACS Publications

© 2021 American Chemical Society

9618

<https://doi.org/10.1021/acs.jpcc.1c01703>
J. Phys. Chem. C 2021, 125, 9618–9629

separations in individual LiFePO₄ cathode particles upon charging and discharging using operando scanning transmission X-ray microscopy (STXM).⁵ At a high discharging rate of 2C, the lithiation is relatively uniform. However, at a lower charging/discharging rate of 0.6C, there is a relatively large Li composition variation and SOC heterogeneity across the particles. The authors also calculated the single-particle C rate at different SOC. The computational results suggest that the (de)lithiation in single particles is faster with increasing global C rate.⁵ Readers are recommended to refer to a more comprehensive review of charge heterogeneity in different cathodes at various length scales.⁷ The SOC heterogeneity depends not only on the extrinsic factors during battery cycling, such as current rates and temperature, but also on electrode intrinsic properties, which can originate from the reaction heterogeneity during an electrode synthesis.⁸ Our recent studies showed that phase transformations during cathode synthesis are highly heterogeneous and exhibit in various forms, which can induce chemical heterogeneity both on the surface and in the bulk of cathode particles.^{8–10} The SOC heterogeneity and chemical reaction heterogeneity can not only induce capacity loss but also give rise to electrode structural and mechanical degradation, such as crack formation in electrode particles, which may undermine the battery cycle life.¹¹ Beyond the single particle scale, mechanical degradation is also heterogeneous across the electrode and shows a depth-dependent feature across the electrode vertically to the current collector.¹² The mixture of active materials, conductive additives, and binder is not perfectly uniform, which may induce a local mismatch between the ionic conductivity and electronic conductivity and further aggravate the chemical and structural heterogeneity.¹³ Therefore, electrode materials show a high heterogeneity at multiple length scales, and it is essential to understand and modulate the electrode heterogeneity to optimize the battery performance.

The SOC heterogeneity and chemical reaction heterogeneity are universal in various electrode materials, which can contribute to the formation of different crystallographic defects in electrode particles.⁷ On the other hand, the crystallographic defects can modify the electrode lattice structure and thus modulate the charging reactions and battery performance.^{10,14–17} For example, Signer et al. studied the nucleation and dynamics of dislocations at different SOCs and illustrated how the formation of partial dislocations promotes the voltage fade in lithium-rich layered oxides.¹⁴ The Bragg coherent diffraction imaging (BCDI) results suggested that the displacement field does not change much upon charging to 4.2 V. At 4.3 V, the authors observed two singularities of the displacement field, indicating the formation of edge dislocations. Charging to a higher voltage (4.4 V) induces additional dislocation formation.¹⁴ Crystallographic defects in electrode particles can be categorized in multiple dimensions, that is, zero-dimensional (0D) point defects (e.g., doping), one-dimensional (1D) line defects (e.g., dislocation), two-dimensional (2D) planar defects (e.g., grain boundaries), and three-dimensional (3D) bulk defects (e.g., voids, cracks).^{18,19} Our recent studies showed that engineering the crystallographic defects and electrode particle microstructure at multiple dimensions can effectively modulate the SOC distribution and enhance battery performance.^{10,15–17} For example, engineering 3D dopant distribution in electrode particles can enhance the performance stability of Ni-rich, Co-free cathodes.^{16,17} Modulating the crystallographic orientation

can guide the charge distribution and improve the battery performance of Ni-rich layered oxide cathodes.¹⁰ We also observed the evolution of microstructural defects in Li- and Na-layered cathodes under Kr ion irradiation and concluded that structural defects can be manipulated using a high-energy ion irradiation.²⁰ Therefore, manipulating the chemical and structural properties of electrode materials at the mesoscale can be an effective and promising approach to modulating battery performance. However, it is not trivial to characterize electrode properties at nanoscale or microscale, especially under operando/in situ conditions. In the last five years, we applied synchrotron X-ray imaging techniques extensively to investigate heterogeneous, defect-rich battery materials.

Synchrotron X-rays are superior to lab-source X-rays because of their continuous high flux and brightness, which enables a higher signal intensity and less data acquisition time.²¹ Conventional X-ray spectroscopy and diffraction techniques acquire ensemble-averaged information based on numerous particles, such as X-ray diffraction (XRD). However, the intraparticle or interparticle variations cannot be well-distinguished after averaging. Synchrotron imaging techniques play a complementary role by directly visualizing and analyzing the particle-by-particle differences at multiple length scales.²² For the acquisition and interpretation of morphological data, 3D imaging is generally favored over 2D imaging, because 2D imaging averages the depth information. Compared to electron microscopy (EM), synchrotron X-ray imaging techniques have the advantage of probing multiple length scales due to the energy tunability of synchrotron X-rays and many available imaging modalities.^{21,23,24} To acquire 3D morphological information with EM, focused ion beam scanning electron microscopy (FIB-SEM) is generally employed, being destructive to the samples.²⁵ Transmission electron microscopy (TEM)-based tomographic reconstruction can also offer nanometric morphological and chemical information about battery particles.²⁶ A wide range of studies identified different types of defects and their effects on the structure and performance of cathode materials using TEM or scanning transmission electron microscopy (STEM).^{27,28} However, its limited field of view has greatly undermined the statistical representativeness of the results, especially when the materials of interest have a large particle size and are heterogeneous, such as practical battery cathode materials. This challenge can be mitigated by either performing TEM measurements on many particles and over different regions of each particle or complementing the TEM measurements with some ensemble-averaged measurements, such as X-ray spectroscopy. We found that a combination of TEM and X-ray spectroscopy can provide critical, statistically significant insights into the surface chemistry of oxide cathodes.^{17,29–32} Synchrotron X-ray imaging techniques can noninvasively obtain 3D or higher-dimensional chemical and structural information, which enables operando/in situ experiments even under practical battery cycling conditions. It is worth noting that the beam damage can potentially deteriorate the sample and bring inaccuracy to the operando/in situ experiments.^{33,34} Such damage can be mitigated by regulating the operation conditions (e.g., increasing X-ray energy³⁵) and modifying operando/in situ cell design.³⁶ The interaction between beam radiation and matter as well as potential beam damage should be considered when designing operando/in situ experiments. Applying synchrotron X-ray imaging techniques to rechargeable batteries, one can correlate the electrochemical perform-

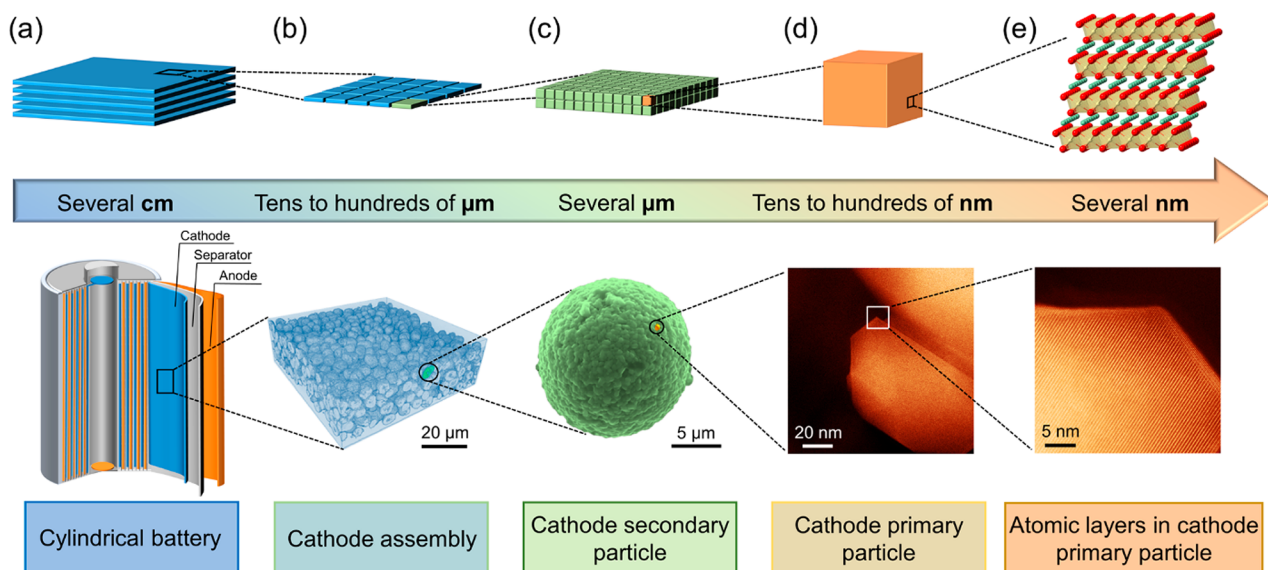


Figure 1. Schematic illustration of the length scales and corresponding battery components. (a) A cylindrical battery of several centimeters. (b) Cathode assembly from tens to hundreds of micrometers.⁵² Copyright 2019 Elsevier. (c) Polycrystalline cathode secondary particle of several micrometers. (d) Cathode primary particle from tens to hundreds of nanometers. (e) Atomic layers in cathode primary particle within several nanometers.

ance with the chemical and structural evolution at multiple length scales in electrodes.²²

2. RECENT PROGRESS IN UNDERSTANDING HETEROGENEITY AND STRUCTURAL DEFECTS IN ACTIVE PARTICLES AND ELECTRODES

A well-functioning Li ion battery with superior electrochemical performance requires the coordination of each component at different length scales. The architecture of Li ion batteries is hierarchical, ranging from the battery-assembly scale in centimeters down to the atomic scale in nanometers (Figure 1). Taking a commercial cylindrical battery as an example, the main components include a cathode, separator, electrolyte, and an anode (Figure 1a). Generally, the cathode has more choices of materials, and the structure is more complicated than other components. The cathode assembly consists of active materials, conductive additives, and a binder (Figure 1b). The active materials are composed of numerous micron-sized particles, which can be either single-crystal particles or polycrystalline secondary particles comprising nanosized single-crystal primary particles oriented randomly or in a certain pattern (Figure 1c,d). Zooming into single-crystal grains, Li ions and transition-metal ions are arranged in an ordered and repeated manner in the lattice. For example, Figure 1e shows the lattice structure of a layered cathode with alternate layers of Li ions and transition-metal ions. Throughout different length scales, many of the local chemical and structural heterogeneities may interfere with global electrode properties and electrochemical performance. Therefore, a comprehensive understanding of the heterogeneity at different length scales is crucial.

2.1. Compositional Heterogeneity. A homogeneous transition-metal ion distribution in cathode particles has been considered as a critical criterion to achieve a decent electrochemical performance of alkali ion batteries. However, our recent studies show that sodium-layered cathode materials with highly 3D heterogeneous transition-metal distributions exhibited good performance.^{37,38} Three cathode materials with

the same chemical formula of $\text{Na}_{0.9}\text{Cu}_{0.2}\text{Fe}_{0.28}\text{Mn}_{0.52}\text{O}_2$ but different transition-metal distributions were synthesized (CFM-Cu, CFM-Mn, and CFM-Fe).²⁷ Among these cathodes, CFM-Cu showed the best performance in Na ion cells with an initial discharge capacity of 125 mAh g^{-1} at 0.1C between 2 and 4 V and no capacity fading after 100 cycles.³⁷ 3D full-field transmission X-ray microscopy (TXM) was used to quantify elemental distributions. TXM is powerful to probe elemental distribution and electronic state (e.g., oxidation state) distribution at a fast data acquisition speed with a resolution of tens of nanometers.²¹ However, potential pitfalls in data analyses should be addressed to avoid data misinterpretation, which will be discussed in the next section. Herein, the elemental association maps of CFM-Cu based on TXM suggested the elemental distribution in a large number of nanodomains deviates from the global stoichiometry ($\text{Na}_{0.9}\text{Cu}_{0.2}\text{Fe}_{0.28}\text{Mn}_{0.52}\text{O}_2$). Specifically, the surface is dominated by single and binary metal associations (Figure 2a), while the bulk mostly comprises ternary metal associations (Figure 2b). This study really opens up a few questions. Are great performing materials in the literature always homogeneous in elemental distributions? This question can essentially be applied to any multielement oxide cathodes. Does the elemental heterogeneity create different charge distributions in battery particles? Can the elemental heterogeneity be designed to benefit battery performance?

We applied the elemental 3D distribution approach to Li ion batteries by introducing dopants as point defects to nanosized single-crystal grains. The dopant distribution can be modulated during the cathode synthesis. We used a multielement-doped cathode material $\text{LiNi}_{0.96}\text{Mg}_{0.02}\text{Ti}_{0.02}\text{O}_2$ (Mg/Ti-LNO) as a platform to investigate the dopant redistribution during synthesis. A combination of X-ray photoelectron spectroscopy (XPS) and Ni K-edge extended X-ray absorption fine structure (EXAFS) wavelet transform analysis suggests that both Mg and Ti are enriched at the surface of the mixed metal hydroxide precursor (schematically represented in Figure 2c). Upon calcination, both Mg and Ti diffuse into the nickel hydroxide

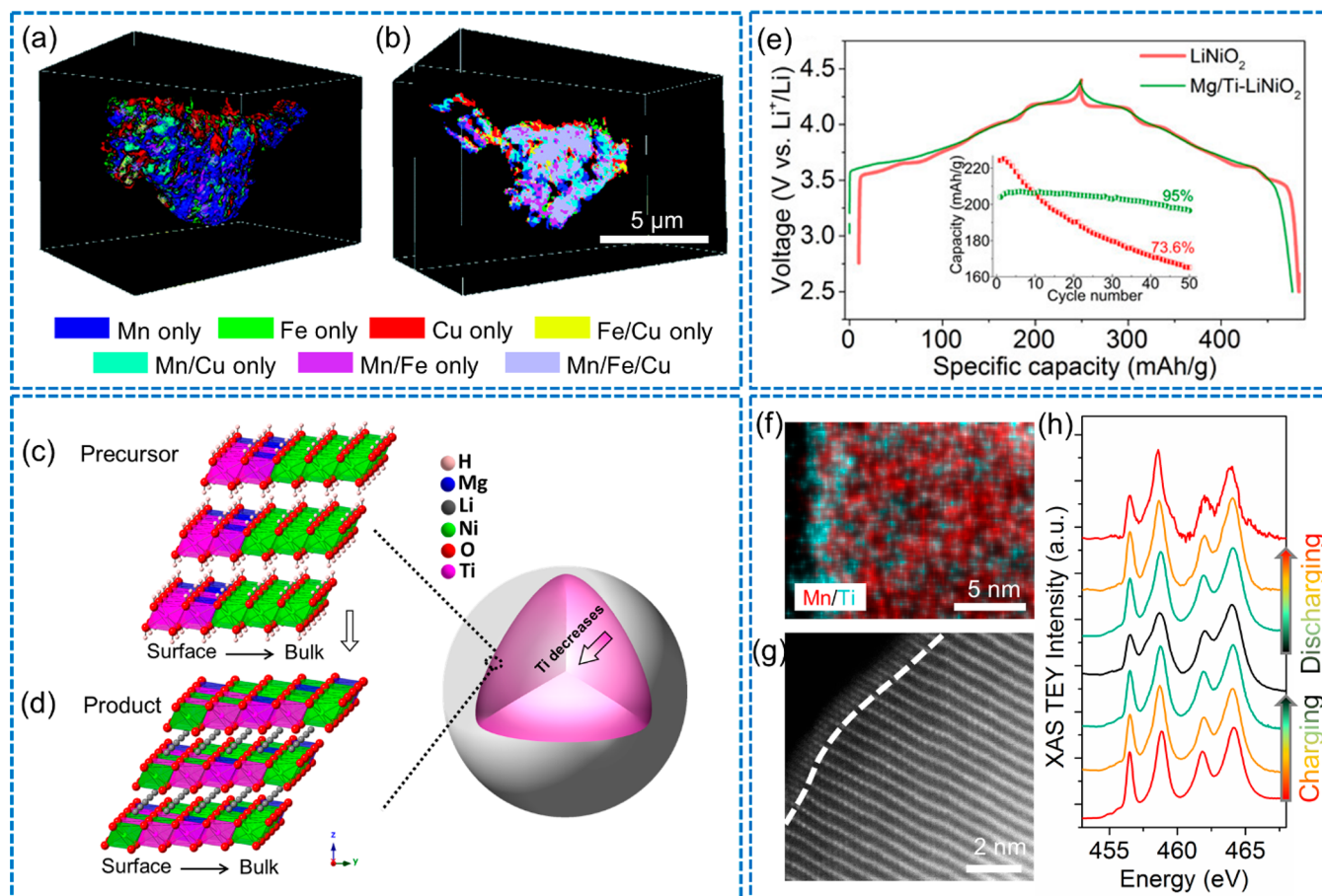


Figure 2. Elemental distribution heterogeneity in various cathode particles at different length scales. (a) 3D elemental association map of pristine $\text{Na}_{0.9}\text{Cu}_{0.2}\text{Fe}_{0.28}\text{Mn}_{0.52}\text{O}_2$ (CFM-Cu) at the particle surface. (b) A selected virtual slice cut through the bulk of the same CFM-Cu particle in (a), the bottom of (a, b) shows the color-coded elemental association.³⁷ Copyright 2018. Royal Society of Chemistry. Schematic illustration of elemental distribution in (c) precursor and (d) product of the Mg/Ti-LNO cathode material.⁸ Copyright 2020. John Wiley and Sons. (e) Voltage profiles of Li cells containing LiNiO_2 and Mg/Ti-LNO at 0.1C (20 mA g⁻¹) and 22 °C within 2.5–4.4 V, where the inset shows the discharge capacity change as a function of cycle number.¹⁶ Copyright 2019. American Chemical Society. (f) STEM-EDS mapping of NMC811-Ti after 300 cycles at 1C within 2.5–4.5 V. (g) STEM image of pristine NMC811-Ti. The dashed line indicates the distinction between the surface reconstruction layer and bulk layered structure. (h) Ti L-edge soft XAS spectra at different SOCs.¹⁷ Copyright 2019. American Chemical Society.

matrix.⁸ After the calcination protocol completes, Mg distributes homogeneously throughout the cathode particle, while Ti is enriched at the particle surface (Figure 2d). The resulting cathode material Mg/Ti-LNO with a 3D hierarchical dopant distribution showed smoother charge and discharge profiles (due to less phase transformation) and higher capacity retention than pure LiNiO_2 under the same operating conditions (Figure 2e).¹⁶ The homogeneously distributed Mg may suppress phase transformations and thereby enhance the bulk structural stability. Meanwhile, the surface-enriched Ti may mitigate the surface oxygen loss by forming strong ionic bonds with O and reducing the hybridization between transition-metal 3d and oxygen 2p orbitals.¹⁶ By applying the 3D dopant distribution approach, we also observed a stability enhancement in other cathode materials such as Ti-doped $\text{LiNi}_{0.8}\text{Mn}_{0.1}\text{Co}_{0.1}\text{O}_2$ (NMC811-Ti).¹⁷ The STEM-energy dispersive X-ray spectroscopy (EDS) mapping of NMC811-Ti implied that Ti was enriched at the cathode particle surface (Figure 2f). The bulk of the particles had a layered structure, while the surface had a deactivated reconstruction layer (Figure 2g). Similar to that observed in Mg/Ti-LNO, the surface-enriched Ti in NMC811-Ti particles also reduced the covalency between transition metals and oxygen.¹⁷ The

chemical environment of Ti is highly reversible upon charging and discharging, which contributes to excellent oxygen reversibility and electrochemical cycling stability (Figure 2h).¹⁷ Overall, our results showed engineering the elemental distribution in individual cathode particles can modulate the global electrochemical performance. However, the electrochemistry within individual particles, such as local charge distribution, was not fully understood. Therefore, we extended our work to further investigate the chemical-electrochemical correlation at the mesoscale.

2.2. Phase Propagation Heterogeneity and SOC Heterogeneity. Most commercial Li ion batteries work based on ion intercalation/deintercalation concurrently with redox reactions in cathodes during discharging or charging. Because of the nonuniformity of redox reactions, SOC distribution heterogeneities can widely exist ranging from individual particles to ensembled electrodes.^{3,7,39} The SOC heterogeneity can be created by different operating conditions during battery cycling or result from intrinsic electrode properties that are related to electrode material synthesis or active material casting and drying.^{5,8,40,41} Recently, we studied the precursor-to-layered oxide phase transformations at different stages of calcination using transition-metal oxidation

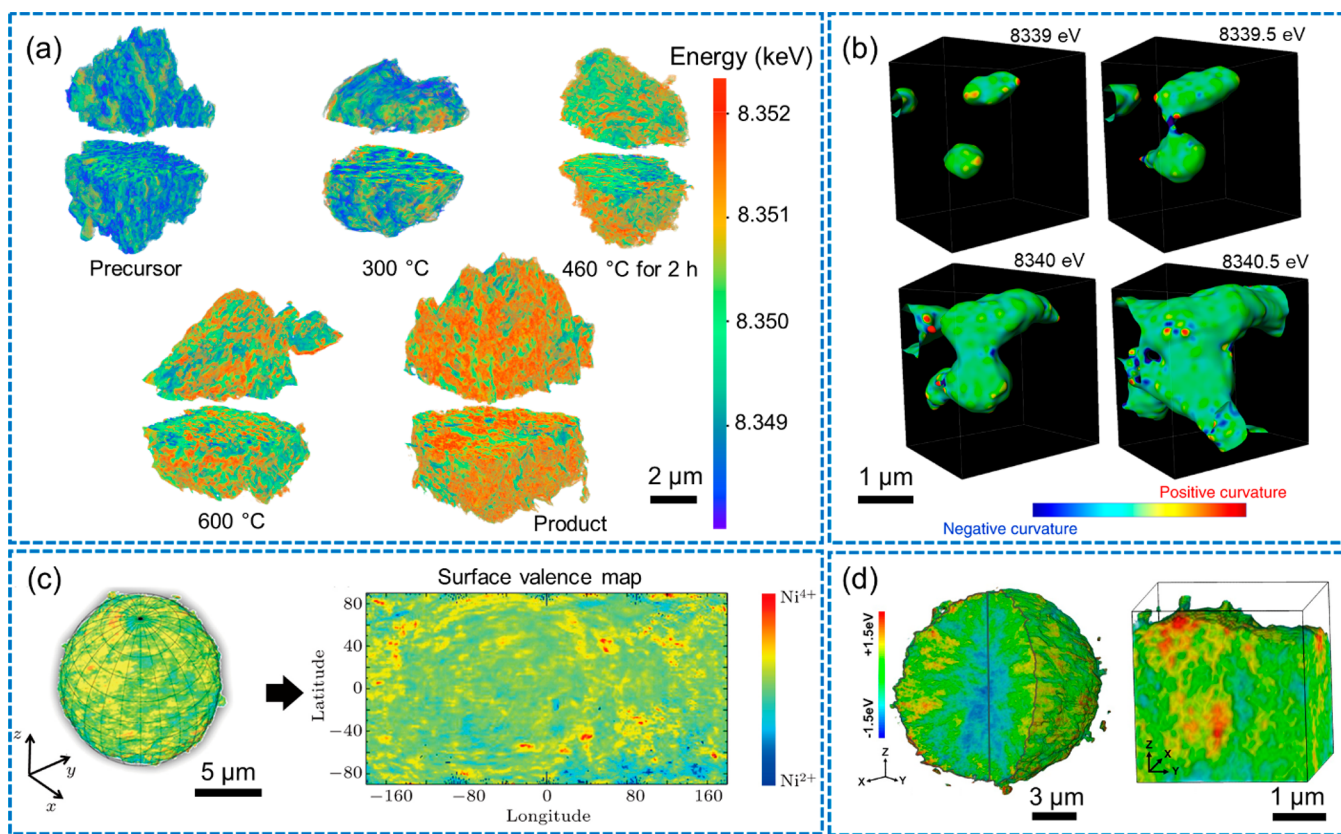


Figure 3. Phase transformation heterogeneity and SOC heterogeneity within various cathode particles at different length scales. (a) Ni K-edge 3D TXM at different states during the calcination of the Mg/Ti-LNO cathode material.⁸ Copyright 2020 John Wiley and Sons. (b) The isosurface evolution and phase front propagation as a function of the Ni K-edge energy.⁴² Copyright 2018 Springer Nature. (c) 3D Ni oxidation state distribution at the surface of NMC811 particle based on full-field hard X-ray spectromicroscopy. The cylindrically projected map is provided for a better visualization.⁹ Copyright 2020 Chinese Physical Society. (d) 3D Ni oxidation state in the bulk of NMC811 particle at the first charged state.¹⁰ Copyright 2020 Springer Nature.

states as a proxy for phase propagation (Figure 3a).⁸ The phase transformations are highly heterogeneous, which exhibit in different forms. The mosaic-like heterogeneity remains throughout the whole calcination process (Figure 3a). On the other hand, there is a radial heterogeneity from the surface to bulk at the early stage of calcination, which becomes trivial in the product.⁸ To further decipher the mechanism of heterogeneous phase transformations in layered cathode materials, we performed *in situ* TXM to map the phase propagation fronts and developed a model to identify the distribution of the parent phase and new phase at the mesoscale under thermal abuse conditions.⁴² In this study, the reductive phase transformations experienced a phase propagation from the new phase (more reduced with lower Ni K-edge energy) to the parent phase (more oxidized with higher Ni K-edge energy).⁴² A localized region was selected to visualize the phase propagations, where the evolution of local valence curvatures at the isosurface was displayed at different Ni K-edge energy (Figure 3b). At the low energy (8339 eV), the sites were discrete, and the positive curvatures dominated. As the phase propagated with the energy increasing to 8339.5 eV, the discrete sites aggregated and formed a joint region with a neck shape (Figure 3b). The necklike region was populated with highly negative curvatures, which implies the new phase domains merged.⁴² As the phase propagation continued to high energy (8340 and 8340.5 eV), the joint region grew, and the necklike feature disappeared eventually. The negative

curvatures at the neck structure mostly turned to neutral/positive curvatures (Figure 3b). The results showed the phase transformations were highly heterogeneous and the initiation of the phase transformation was potentially more rapid at grain boundaries and surface.⁴² The reaction heterogeneity during the electrode material synthesis may lead to a chemical heterogeneity in electrode particles.⁸ Jiang et al. revealed the chemical inhomogeneity at the surface of polycrystalline cathode particles using a combination of soft X-ray nanoprobe and hard X-ray nanoresolution spectro-tomography.⁹ The Ni oxidation state map over the entire NMC811 cathode particle surface exhibited a high degree of inhomogeneity, and the deeply charged domains (represented by red regions) and deeply discharged domains (represented by blue regions) tended to be isolated (Figure 3c). It is worth noting that the charge distribution analysis and degradation at the particle surface should be location-sensitive. Therefore, statistical analyses are suggested to be taken for the surface-sensitive ultrahigh resolution techniques to validate the representativeness of selected regions. Furthermore, we observed a high degree of Ni oxidation state heterogeneity in the bulk of NMC811 cathode particle at the first charged state (Figure 3d).¹⁰ With advanced synchrotron X-ray microspectroscopic imaging tools, we were able to resolve the SOC heterogeneity in different electrodes at multiple length scales. To comprehensively understand the battery working and failure

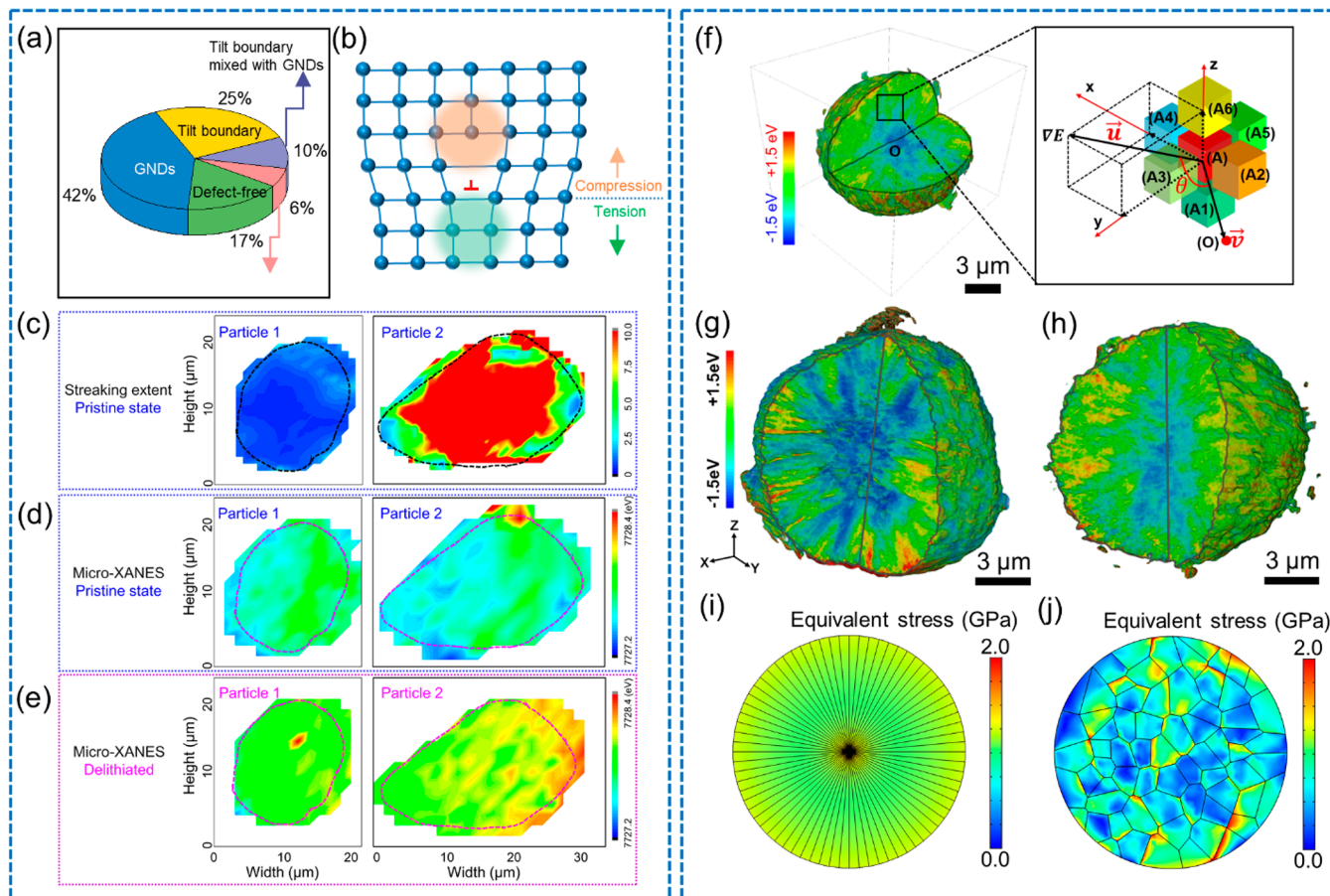


Figure 4. Defect engineering and crystallographic orientation modulating at mesoscale. (a) Percentage of each defect in LiCoO₂ particles based on 37 particles (over 10 000 Laue diffraction patterns). (b) Schematic illustration of dislocation within electrode particles. (c) Streaking extent based on LXMD of particle 1 and particle 2 at pristine state. The charge distribution based on Co K-edge micro-XANES of particle 1 and particle 2 (d) at pristine state and (e) after in situ chemical delithiation. The dashed lines in (c–e) define the areas for study.¹⁵ Copyright 2020 John Wiley and Sons. (f) Schematic illustration of the valence gradient model for Ni oxidation state distribution analysis. Ni oxidation state distribution in the (g) rod-NMC and (h) gravel-NMC particles at the first charged state. Here the Ni oxidation state is represented by the relative energy shift of the Ni K-edge XAS. The equivalent stress of (i) rod-NMC and (j) gravel-NMC at 100% SOC. Compared with rod-NMC, the stress is more heterogeneous and concentrated at the grain boundaries in gravel-NMC.¹⁰ Copyright 2020 Springer Nature.

mechanisms, further correlation of the SOC distribution with structural evolutions is demanded.

2.3. Microstructural Heterogeneity. The chemical heterogeneity and SOC heterogeneity can originate from microstructural heterogeneity, and thus manipulation of the microstructure can, in turn, modulate the electrochemical performance.^{14,43} Our recent study has shown that different types of crystallographic defects exist in individual grains of layered cathodes.¹⁵ Specifically, four categories of defects, namely, geometrically necessary dislocations (GNDs), tilt boundary, tilt boundary mixed with GNDs, and stacking tilt boundaries, were quantified to share 42%, 25%, 10%, and 17% of defect-present Laue diffraction patterns (Figure 4a). We then chose the particles that have only GNDs to investigate the correlation with redox reactions, charge distribution, and density of GNDs in battery cathode materials using in situ Laue X-ray microdiffraction (LXMD) and synchrotron X-ray spectroscopic imaging techniques (Figure 4b). LXMD can identify the location of different crystallographic defects at the mesoscale. Combined with spectroscopic imaging, the structural and chemical properties can be correlated, whereas, given the high resolution, the data representativeness should be evaluated. Herein, two representative particles with increasing

streaking extent (from particle 1 to particle 2, Figure 4c) identified by LXMD patterns are in situ chemically delithiated to a low SOC. Co K α fluorescence mapping, LXMD, and micro-X-ray absorption near-edge structure (XANES) are performed for both pristine and in situ delithiated samples.¹⁵ In its pristine state, Co has a relatively low oxidation state in both particles (Figure 4d). After chemical delithiation, particle 2 with a larger streaking extent (higher density of GNDs) shows a higher Co oxidation state, which implies GNDs can promote delithiation during the initial charging (Figure 4e).¹⁵ Our further study discovered that high-energy ion radiation can create dislocations controllably in both density and distribution in Li- and Na-layered cathodes.²⁰ We expect that controlling structural defects through high-energy ion radiation can offer an effective path toward tailoring electrochemical properties of battery materials. In addition, a Ni–Li antisite defect is universally observed in layer oxide cathodes during synthesis and electrochemical cycling, which hinders Li transport and reduces capacity.⁴⁴ Recently, Lin et al. identified that Ni–Li antisite defect-rich regions can serve as nucleation sites for promoting the formation of intragranular cracks in Ni-rich layered cathodes.²⁷ Furthermore, a typical planar defect, that is, stacking faults, is one of the origins of the

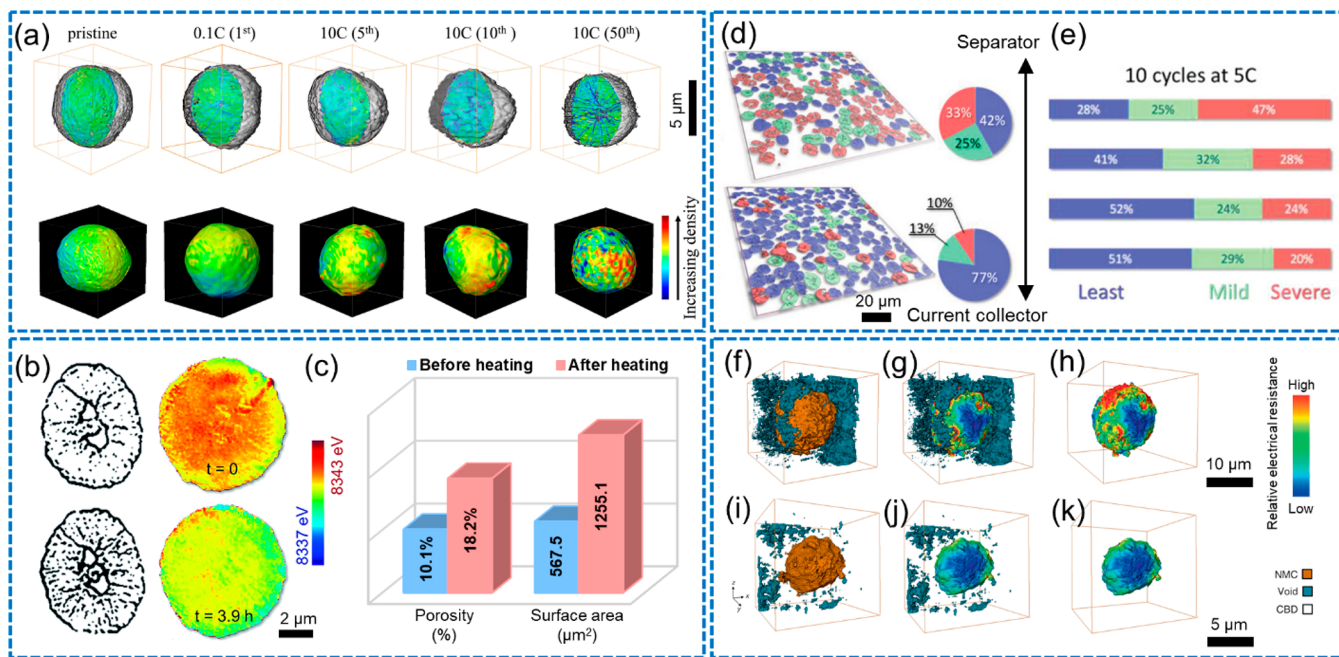


Figure 5. Morphological defects and heterogeneous damage in various cathode particles at different length scales. (a) 3D rendering showing the cracks in the bulk and corresponding electron traffic map over the surface of particles after different cycling history.⁵⁰ Copyright 2018 Elsevier. (b) Chemical evolution and segmentation of the cracks with different exposure durations to thermal abuse at 380 °C. (c) Quantitative analyses of porosity and surface area before and after being heated at 380 °C for ~4 h.⁵¹ Copyright 2018 Royal Society of Chemistry. (d) Different extent of damage on the first layer of particles near separator side (top) and near current collector side (bottom) after 10 cycles at 5C. (e) Fracturing profiles across the electrode after 10 cycles at 5C.⁵² Copyright 2019 John Wiley and Sons. (f, i) 3D rendering of two regions of interest showing the distribution of NMC, void, and CBD. (g, j) 3D rendering of calculated local relative electrical resistance distribution. (h, k) The same particles in (g, j) without showing voids.⁵³ Copyright 2020 Springer Nature.

electrochemical irreversibility and sluggish Li diffusion in Li-rich layered oxides.^{14,45} Synthetic control is crucial to regulate those defects and enhance the electrochemical performance.^{46,47}

Beyond manipulating defects within single grains, we found that charge distribution and chemomechanical properties can be modulated through architecting the grain crystallographic orientation of polycrystalline battery cathode particles.¹⁰ We developed a mathematical model to quantitatively analyze the correlation between charge distribution and crystallographic orientations (Figure 4f). Specifically, a valence gradient vector was defined to dictate the Ni oxidation state difference between the central voxel and its surrounding six voxels, which had their own local Ni oxidation states determined by TXM. By summing the partial valence gradient vectors along x , y , and z directions, a total valence gradient vector (\mathbf{u}) can be obtained. Another vector \mathbf{v} was defined by connecting the central voxel to the gravity center of the particle. The angle θ between \mathbf{u} and \mathbf{v} is an indicator for distinguishing different charge distribution patterns, and the size of \mathbf{u} increases with a higher charge heterogeneity between two voxels. On the basis of the developed valence gradient model, we evaluated two types of NMC811 cathodes with two grain crystallographic orientations, namely, rod-NMC (Figure 4g) and gravel-NMC (Figure 4h), and quantitatively analyzed the charge distributions in the two cathodes. More valence gradient vectors with $\theta \approx 90^\circ$ are identified in rod-NMC than gravel-NMC, which is a fingerprint for the radially aligned Ni oxidation state (Figure 4g).¹⁰ In contrast, gravel-NMC shows a relatively random Ni oxidation state distribution (Figure 4h). In collaboration with the Zhao group at Purdue, using the finite element modeling,

we found less stress buildup between the grains in rod-NMC than in gravel-NMC, which can be potentially attributed to the cooperative alignment of the grains (Figure 4i,j). It has been reported that hollow particles are more resistant to stress-induced cracks compared to solid particles, which suggests another effective strategy of morphology manipulation to mitigate mechanical degradation.⁴⁸ To summarize, our recent studies have shown that manipulating microstructure and engineering structural defect within electrode particles can modulate local charge distributions, which provides a bottom-up approach to enhance battery performance from the single-particle scale.

2.4. Chemomechanical Interplay and Heterogeneous Damage at Multiple Length Scales. The prevailing SOC heterogeneity in rechargeable battery electrodes, coupled with crystallographic defects and phase transformations, may induce hot spots of mechanical stress and lead to a chemomechanical breakdown of electrodes, such as crack formation.⁴⁹ The cracks lead to poor electronic conductivity and expose more fresh surface of electrode particles, which induces more side reactions between the electrode and electrolyte and deteriorates the battery performance eventually.¹¹ Understanding the chemomechanical interplay in electrodes is critical to enhancing electrode integrity and battery cycling stability. Synchrotron X-ray imaging techniques coupled with mechanical analysis enable the visualization and quantification of chemomechanical interplay at multiple length scales. For example, in collaboration with the Liu group at the SLAC National Accelerator Laboratory, we reported the mesoscale morphological evolution of $\text{LiNi}_{0.6}\text{Mn}_{0.2}\text{Co}_{0.2}\text{O}_2$ (NMC622) secondary particles that are caused by a chemomechanical

degradation at different charging rates and correlated with SOCs.⁵⁰ Using a combination of 3D X-ray tomography and simulation, we observed that more cracks formed in cathode particles upon cycling at a high charging rate, leading to a more heterogeneous local current distribution (Figure 5a). High charging rates may exacerbate heterogeneous charge distributions, leading to a more aggressive buildup of local stress.

A chemomechanical breakdown is generally more prominent and detrimental in extreme environments, such as thermal abuse conditions. A thorough understanding of chemomechanical interplay under thermal abuse conditions can also create insights into studying battery failure.⁵¹ Wei et al. correlated the chemical evolution and mechanical degradation of charged NMC622 particles under thermal abuse conditions.⁵¹ The operando heating Ni K-edge XANES mapping results suggest Ni reduction upon heating, and the *in situ* nanotomography implied more radial crack formation after thermal abuse (Figure 5b). The authors further quantified the microstructural properties. The results showed that both porosity and surface area were dramatically increased upon heating (Figure 5c). These results collectively suggest that the chemical and mechanical evolutions are closely correlated at the mesoscale. Beyond the single-particle scale, the electrode-scale chemomechanical interplay also plays a significant role in determining battery performance.⁵² The application of X-ray phase contrast nanotomography enables the probing of thousands of cathode active material particles in the electrode ensemble simultaneously.¹² The extent of damage of different particles was categorized as least damaged, mildly damaged, and severely damaged.¹² The statistical analysis showed different extents of damage across the electrode (Figure 5d). Specifically, more active particles were severely damaged near the separator side (33%) than near the current collector side (10%, Figure 5d). After 10 cycles at 5C, severely damaged particles increased in both near separator regions and near current collector regions, and the damage pattern was depth-dependent across the electrode (Figure 5e). In practical electrode assemblies, active materials are embedded in the carbon/binder domain (CBD), which further complicates the charge distribution scenario. On the basis of the machine-learning-assisted analysis, Liu and co-workers investigated over 650 active particles through phase-contrast X-ray tomography to identify the detachment of CBD from active particles.¹³ The CBD network attached to active particles provided paths for electron transfer. The voids between CBD and active particles were infiltrated with electrolytes, which enabled Li ions to diffuse (Figure 5f,i). Partial CBD detachment creates more voids around the active particle (Figure 5f), leading to a more severe and heterogeneous local electrical resistance at the active particle surface (Figure 5g,h). In contrast, electrical resistance was less accumulated for the active particle with less CBD detachment (Figure 5j,k). The CBD detachment and nonuniform voids distribution induce a mismatch between ionic conductivity and electronic conductivity, which compromises the effective utility of active particles. Furthermore, the electrode fabrication process can introduce additional heterogeneity. For example, the motions of active material particles in the electrode assembly during the electrode solidification were measured using a combination of fast X-ray microtomography (FXT) and a special data analysis method.⁴¹ In collaboration with the Xiao group at Brookhaven National Laboratory, we found that the particle motion was highly geometric location-dependent and that tuning the

solvent evaporation rate to optimize the motion of active material particles was crucial to obtain a high-quality electrode assembly.⁴¹ In summary, the chemical, structural, and mechanical heterogeneities are prevalent in electrode materials from the atomic scale up to the electrode assembly. Properly regulating the electrode heterogeneities can effectively optimize the overall battery performance.

3. POTENTIAL PITFALLS AND STRATEGIES TO MITIGATE

Synchrotron imaging techniques serve well to probe various chemical and structural properties of battery materials at multiple length scales thanks to the high energy and resolution capabilities. In the meantime, the inappropriate data interpretation and high resolution-induced unrepresentativeness can potentially bring bias to understanding materials properties. Herein, we provide a few examples of synchrotron characterization data analysis and discuss the significance of legitimate data interpretation.

The quantity of raw data for synchrotron imaging characterizations is usually enormous, and processing these data involves complicated computational algorithms. As a state-of-the-art synchrotron imaging technique that is widely used in characterizing energy storage materials, TXM is taken as an example to illustrate the potential concerns and strategies of data processing. To obtain chemical mapping, a typical TXM data process procedure involves multiple steps such as tomographic reconstruction, image rescaling and alignment, spectra filtration, edge energy or white-line energy determination, least-squares linear combination fitting, and data analysis and potential mathematical modeling.^{53,54} Depending on the algorithms, each of the aforementioned steps can potentially generate artifacts and errors that may interfere with the ultimate chemical mapping results. However, a universal protocol for data processing and a standard of error tolerance has not been established yet. Therefore, great caution should be taken during data processing, and error analysis is highly recommended for data interpretation.

A potential concern of nanometer-scale or micron-scale imaging techniques is if the measured region of interest (ROI) is representative of the entire bulk material. Taking rechargeable battery electrode materials as an example, a Li ion battery cathode ensemble is composed of numerous cathode particles, and the heterogeneity of materials properties may exist within a single particle and among particles. For characterizations performed at the single-particle scale, it is essential to evaluate if the phenomenon observed can be generally applied to the entire electrode assembly. To avoid misleading results, measurements and analyses based on a large number of particles are recommended. Some of our collaborative studies can well-represent our efforts in this direction. For example, Yang et al. performed hard X-ray phase-contrast tomography, which enables the simultaneous acquisition of chemomechanical information on thousands of particles and statistical analyses of the entire electrode.¹²

To interpret the enormous amount of data, an emerging frontier is to apply machine learning for statistical analyses. Our group participated in a number of studies using machine learning methods for TXM data analysis led by the Liu group at the SLAC National Accelerator Laboratory. Jiang et al. reported a machine learning-based segmentation approach to quantify the degree of detachment of over 650 NMC811 cathode particles, which showed superior data reliability to the

conventional segmentation method.¹³ Mao et al. classified and quantified different SOC domains of NMC622 cathode particles within different voltage windows using a hybrid supervised and unsupervised machine-learning approach.⁴⁸ Besides, the machine learning-assisted analysis can reveal additional information that conventional analyses are not able to approach. For example, Zhang et al. identified the functionally important minority phases of over 100 LiCoO₂ cathode particles under battery operating conditions with data-mining approaches.⁵⁵

Considering the limited allocated beamtime and potential time-consuming experimental design for synchrotron imaging characterizations, it is not always feasible to acquire enough particles for statistical analyses of 3D measurements. Therefore, 2D measurements are recommended as a complement to 3D measurements because the data acquisition time is much shorter for 2D measurements, and thus information on more particles can be acquired. Our recent study demonstrated such a 3D/2D combined effort to understand the phase propagation from metal hydroxide precursor to layered oxides.⁸ In addition, a direct comparison of the selected ROI and the entire bulk material is preferred to verify the data representativeness. For example, Xu et al. compared the particle volume, particle size, and neighbor distance of representative volume element (RVE) with the entire electrode to ensure the selected RVE is statistically representative of the heterogeneous damage in the entire electrode.⁵² Furthermore, complementary characterization tools at different length scales should always be considered whenever possible to eliminate the potential bias. For example, Singer et al. performed synchrotron powder diffraction on the ensemble-averaged electrode to confirm the dislocations in the selected particles identified by operando BCDI are representative.¹⁴ Overall, drawing a universal conclusion for a large-scale ensemble from a limited set of individual particles can potentially be problematic and misleading to some degree. Given the multiscale heterogeneity we discussed in this Perspective, data representativeness should always be put on top of the mind when designing and performing high-resolution imaging experiments at small scales.

4. CONCLUSION AND OUTLOOK

Multiscale chemical and structural heterogeneities widely exist in various electrode materials, and we find properly regulating these heterogeneities can improve battery performance. We show that engineering elemental distributions in electrode particles can enhance the structural stability of both the surface and bulk of electrode particles. Further correlating the chemical evolution with local electrochemical change, we find the SOC distribution is highly heterogeneous at the surface and in the bulk of electrode particles, which can result from extrinsic battery operation conditions as well as originate from the intrinsic electrode properties associated with heterogeneous chemical reactions during synthesis. The SOC heterogeneity can give rise to defect formation in electrode particles. Alternately, engineering structural defects within electrode particles can modulate charge transport and enhance global electrochemical performance. The manipulation of the microstructure of electrode particles, such as engineering crystallographic orientation, has become an emerging approach to efficiently increase battery energy density without changing chemical compositions or global crystal structures of electrode materials. Heterogeneous SOC distribution and phase trans-

formations can give rise to mechanical degradations, such as crack formation. Given the chemical, structural, and mechanical heterogeneities throughout the electrodes we have studied, we emphasize the importance of regulating multiscale heterogeneities and structural defects and provide several promising approaches to enhance battery performance in a bottom-up manner. We highlight that it is crucial to ensure the data representativeness when evaluating local materials properties. To make characterization results practically relevant, it is crucial to perform characterizations on battery materials that show typical battery performance. Efforts should be made, if possible, to avoid making conclusions from characterizing poorly synthesized, low-performance, less representative materials.

From the technical standpoint, the application of synchrotron X-ray imaging techniques in rechargeable batteries gives rise to an unprecedented understanding of chemical and structural interplay at multiple length scales. On the other hand, the emerging needs for probing more fundamental battery mechanisms drive the characterization tools toward more advanced functions.⁵⁶ With the rapid development of synchrotron source and instruments, higher spatial and temporal resolutions as well as signal-to-noise ratio will be obtained, which pave the way for materials characterizations at smaller length scales and under ultrafast operation conditions.^{57–59} An emerging trend of understanding rechargeable battery operation and failure mechanism is to probe the interplay of electrochemical-chemical-structural properties at different length and time scales using a combination of multiple characterization tools, such as the combination of X-ray CT, spectroscopic imaging tools, and X-ray diffraction. In the future, synchrotron X-ray imaging techniques that are coupled with more characterizations are worth exploring.^{60,61} In addition, X-ray ptychography is a promising imaging technique with a high spatial resolution that takes the advantages of both STXM and coherent diffraction imaging (CDI), which is powerful to resolve various structural properties in energy storage materials.⁶² Furthermore, interdisciplinary studies will provide further insights into data interpretation and fundamental understanding of materials properties, with machine learning-assisted analysis being a typical example applied in materials science recently.^{63,64}

■ AUTHOR INFORMATION

Corresponding Author

Feng Lin – Department of Chemistry, Virginia Tech, Blacksburg, Virginia 24061, United States;  orcid.org/0000-0002-3729-3148; Email: fenglin@vt.edu

Author

Zhijie Yang – Department of Chemistry, Virginia Tech, Blacksburg, Virginia 24061, United States

Complete contact information is available at:
<https://pubs.acs.org/10.1021/acs.jpcc.1c01703>

Notes

The authors declare no competing financial interest.

Biographies



Zhijie Yang is currently a PhD student in Chemistry at Virginia Tech. He obtained his Bachelor's degree from South China University of Technology (SCUT) in 2018. His research interest is in understanding and developing advanced layered oxide cathode materials for Li-ion batteries.



Dr. Feng Lin is currently an Assistant Professor of Chemistry, with courtesy appointments in the Department of Materials Science & Engineering and in the Macromolecules Innovation Institute at Virginia Tech. He holds a Bachelor's degree in Materials Science and Engineering (2009) from Tianjin University, and an MSc degree (2011) and a PhD degree (2012) in Materials Science from Colorado School of Mines. Prior to Virginia Tech, Feng worked at QuantumScape Corporation as a Senior Member of Technical Staff (2015–2016), Lawrence Berkeley National Laboratory as a Postdoctoral Fellow (2013–2015), and National Renewable Energy Laboratory as a Graduate Research Assistant (2010–2012). His research team investigates application-driven fundamental questions in energy storage, catalysis, and smart windows.

ACKNOWLEDGMENTS

The authors acknowledge the funding agencies in supporting different aspects of the work presented here. The Co-free cathode work is supported by the U.S. Department of Energy (DOE) Office of Energy Efficiency and Renewable Energy (EERE) under the Award No. DE-EE0008444. The mechanical study of layered cathodes is supported by the National Science Foundation under Grant No. DMR-1832613. The authors also appreciate the support from synchrotron facilities. The use of SSRL, SLAC National Accelerator Laboratory, is supported by the U.S. DOE, Office of Science, Office of Basic Energy Sciences under Contract No. DE-AC02-76SF00515. This research also used 18-ID of the National Synchrotron

Light Source II, a U.S. DOE Office of Science User Facility operated for the DOE Office of Science by Brookhaven National Laboratory under Contract No. DE-SC0012704. The authors thank the Lin lab members who contributed to the original scientific content of this Perspective. The authors are grateful for the support from collaborators in these studies. F.L. expresses his gratitude to R. Ng Man-tat for exemplifying the spirit of utmost professionalism.

REFERENCES

- (1) Nagaura, T.; Tozawa, K. Lithium Ion Rechargeable Battery. *Prog. Batter. Sol. Cells* **1990**, *9*, 209–219.
- (2) Xu, Y.; Hu, E.; Zhang, K.; Wang, X.; Borzenets, V.; Sun, Z.; Pianetta, P.; Yu, X.; Liu, Y.; Yang, X. Q.; et al. In Situ Visualization of State-of-Charge Heterogeneity within a LiCoO₂ Particle That Evolves upon Cycling at Different Rates. *ACS Energy Lett.* **2017**, *2* (5), 1240–1245.
- (3) Tian, C.; Xu, Y.; Nordlund, D.; Lin, F.; Liu, J.; Sun, Z.; Liu, Y.; Doeff, M. Charge Heterogeneity and Surface Chemistry in Polycrystalline Cathode Materials. *Joule* **2018**, *2* (3), 464–477.
- (4) Liu, H.; Strobridge, F. C.; Borkiewicz, O. J.; Wiaderek, K. M.; Chapman, K. W.; Chupas, P. J.; Grey, C. P. Capturing Metastable Structures during High-Rate Cycling of LiFePO₄ Nanoparticle Electrodes. *Science* **2014**, *344* (6191), 1252817.
- (5) Lim, J.; Li, Y.; Alsem, D. H.; So, H.; Lee, S. C.; Bai, P.; Cogswell, D. A.; Liu, X.; Jin, N.; Yu, Y. S.; et al. Origin and Hysteresis of Lithium Compositional Spatiodynamics within Battery Primary Particles. *Science* **2016**, *353* (6299), 566–571.
- (6) Yu, Y.-S.; Kim, C.; Liu, Y.; van der Ven, A.; Meng, Y. S.; Kostecki, R.; Cabana, J. Nonequilibrium Pathways during Electrochemical Phase Transformations in Single Crystals Revealed by Dynamic Chemical Imaging at Nanoscale Resolution. *Adv. Energy Mater.* **2015**, *5* (7), 1402040.
- (7) Zhang, Y.; Yang, Z.; Tian, C. Probing and Quantifying Cathode Charge Heterogeneity in Li Ion Batteries. *J. Mater. Chem. A* **2019**, *7*, 23628.
- (8) Yang, Z.; Mu, L.; Hou, D.; Rahman, M. M.; Xu, Z.; Liu, J.; Nordlund, D.; Sun, C.; Xiao, X.; Lin, F. Probing Dopant Redistribution, Phase Propagation, and Local Chemical Changes in the Synthesis of Layered Oxide Battery Cathodes. *Adv. Energy Mater.* **2021**, *11*, 2002719.
- (9) Jiang, Z.-S.; Li, S.-F.; Xu, Z.-R.; Nordlund, D.; Ohldag, H.; Pianetta, P.; Lee, J.-S.; Lin, F.; Liu, Y.-J. Revealing the Inhomogeneous Surface Chemistry on the Spherical Layered Oxide Polycrystalline Cathode Particles. *Chin. Phys. B* **2020**, *29* (2), 26103.
- (10) Xu, Z.; Jiang, Z.; Kuai, C.; Xu, R.; Qin, C.; Zhang, Y.; Rahman, M. M.; Wei, C.; Nordlund, D.; Sun, C. J.; et al. Charge Distribution Guided by Grain Crystallographic Orientations in Polycrystalline Battery Materials. *Nat. Commun.* **2020**, *11* (83), 1–9.
- (11) Xu, Z.; Rahman, M. M.; Mu, L.; Liu, Y.; Lin, F. Chemomechanical Behaviors of Layered Cathode Materials in Alkali Metal Ion Batteries. *J. Mater. Chem. A* **2018**, *6*, 21859.
- (12) Yang, Y.; Xu, R.; Zhang, K.; Lee, S.; Mu, L.; Liu, P.; Waters, C. K.; Spence, S.; Xu, Z.; Wei, C.; et al. Quantification of Heterogeneous Degradation in Li-Ion Batteries. *Adv. Energy Mater.* **2019**, *9* (25), 1900674.
- (13) Jiang, Z.; Li, J.; Yang, Y.; Mu, L.; Wei, C.; Yu, X.; Pianetta, P.; Zhao, K.; Cloetens, P.; Lin, F.; et al. Machine-Learning-Revealed Statistics of the Particle-Carbon/Binder Detachment in Lithium-Ion Battery Cathodes. *Nat. Commun.* **2020**, *11*, 2310.
- (14) Singer, A.; Zhang, M.; Hy, S.; Cela, D.; Fang, C.; Wynn, T. A.; Qiu, B.; Xia, Y.; Liu, Z.; Ulvestad, A.; et al. Nucleation of Dislocations and Their Dynamics in Layered Oxide Cathode Materials during Battery Charging. *Nat. Energy* **2018**, *3* (8), 641–647.
- (15) Xu, Z.; Hou, D.; Kautz, D. J.; Liu, W.; Xu, R.; Xiao, X.; Lin, F. Charging Reactions Promoted by Geometrically Necessary Dislocations in Battery Materials Revealed by In Situ Single-Particle Synchrotron Measurements. *Adv. Mater.* **2020**, *32* (37), 2003417.

(16) Mu, L.; Zhang, R.; Kan, W. H.; Zhang, Y.; Li, L.; Kuai, C.; Zydlewski, B.; Rahman, M. M.; Sun, C.-J.; Sainio, S.; et al. Dopant Distribution in Co-Free High-Energy Layered Cathode Materials. *Chem. Mater.* **2019**, *31* (23), 9769–9776.

(17) Steiner, J. D.; Cheng, H.; Walsh, J.; Zhang, Y.; Zydlewski, B.; Mu, L.; Xu, Z.; Rahman, M. M.; Sun, H.; Michel, F. M.; et al. Targeted Surface Doping with Reversible Local Environment Improves Oxygen Stability at the Electrochemical Interfaces of Nickel-Rich Cathode Materials. *ACS Appl. Mater. Interfaces* **2019**, *11* (41), 37885–37891.

(18) Zhang, Y.; Tao, L.; Xie, C.; Wang, D.; Zou, Y.; Chen, R.; Wang, Y.; Jia, C.; Wang, S. Defect Engineering on Electrode Materials for Rechargeable Batteries. *Adv. Mater.* **2020**, *32*, 1905923.

(19) Liu, H.; Wolf, M.; Karki, K.; Yu, Y. S.; Stach, E. A.; Cabana, J.; Chapman, K. W.; Chupas, P. J. Intergranular Cracking as a Major Cause of Long-Term Capacity Fading of Layered Cathodes. *Nano Lett.* **2017**, *17* (6), 3452–3457.

(20) Rahman, M. M.; Chen, W.-Y.; Mu, L.; Xu, Z.; Xiao, Z.; Li, M.; Bai, X.-M.; Lin, F. Defect and Structural Evolution under High-Energy Ion Irradiation Informs Battery Materials Design for Extreme Environments. *Nat. Commun.* **2020**, *11*, 4548.

(21) Lin, F.; Liu, Y.; Yu, X.; Cheng, L.; Singer, A.; Shpyrko, O. G.; Xin, H. L.; Tamura, N.; Tian, C.; Weng, T.-C.; et al. Synchrotron X-Ray Analytical Techniques for Studying Materials Electrochemistry in Rechargeable Batteries. *Chem. Rev.* **2017**, *117* (21), 13123–13186.

(22) Wang, L.; Wang, J.; Zuo, P. Probing Battery Electrochemistry with In Operando Synchrotron X-Ray Imaging Techniques. *Small Methods* **2018**, *2* (8), 1700293.

(23) Chueh, W. C.; El Gabaly, F.; Sugar, J. D.; Bartelt, N. C.; McDaniel, A. H.; Fenton, K. R.; Zavadil, K. R.; Tyliszczak, T.; Lai, W.; McCarty, K. F. Intercalation Pathway in Many-Particle LiFePO₄ Electrode Revealed by Nanoscale State-of-Charge Mapping. *Nano Lett.* **2013**, *13* (3), 866–872.

(24) Shapiro, D. A.; Yu, Y. S.; Tyliszczak, T.; Cabana, J.; Celestre, R.; Chao, W.; Kaznatcheev, K.; Kilcoyne, A. L. D.; Maia, F.; Marchesini, S.; et al. Chemical Composition Mapping with Nanometre Resolution by Soft X-Ray Microscopy. *Nat. Photonics* **2014**, *8* (10), 765–769.

(25) Groeber, M. A.; Haley, B. K.; Uchic, M. D.; Dimiduk, D. M.; Ghosh, S. 3D Reconstruction and Characterization of Polycrystalline Microstructures Using a FIB-SEM System. *Mater. Charact.* **2006**, *57* (4–5), 259–273.

(26) Lin, F.; Nordlund, D.; Weng, T. C.; Zhu, Y.; Ban, C.; Richards, R. M.; Xin, H. L. Phase Evolution for Conversion Reaction Electrodes in Lithium-Ion Batteries. *Nat. Commun.* **2014**, *5* (1), 1–9.

(27) Lin, Q.; Guan, W.; Zhou, J.; Meng, J.; Huang, W.; Chen, T.; Gao, Q.; Wei, X.; Zeng, Y.; Li, J.; et al. Ni-Li Anti-Site Defect Induced Intragranular Cracking in Ni-Rich Layer-Structured Cathode. *Nano Energy* **2020**, *76*, 105021.

(28) Li, S.; Yao, Z.; Zheng, J.; Fu, M.; Cen, J.; Hwang, S.; Jin, H.; Orlov, A.; Gu, L.; Wang, S.; et al. Direct Observation of Defect-Aided Structural Evolution in a Nickel-Rich Layered Cathode. *Angew. Chem., Int. Ed.* **2020**, *59* (49), 22092–22099.

(29) Lin, F.; Markus, I. M.; Nordlund, D.; Weng, T.-C.; Asta, M. D.; Xin, H. L.; Doeff, M. M. Surface Reconstruction and Chemical Evolution of Stoichiometric Layered Cathode Materials for Lithium-Ion Batteries. *Nat. Commun.* **2014**, *5* (1), 3529.

(30) Lin, F.; Nordlund, D.; Markus, I. M.; Weng, T.-C. C.; Xin, H. L.; Doeff, M. M. Profiling the Nanoscale Gradient in Stoichiometric Layered Cathode Particles for Lithium-Ion Batteries. *Energy Environ. Sci.* **2014**, *7* (9), 3077–3085.

(31) Mu, L.; Feng, X.; Kou, R.; Zhang, Y.; Guo, H.; Tian, C.; Sun, C.-J.; Du, X.-W.; Nordlund, D.; Xin, H. L.; et al. Deciphering the Cathode-Electrolyte Interfacial Chemistry in Sodium Layered Cathode Materials. *Adv. Energy Mater.* **2018**, *8* (34), 1801975.

(32) Steiner, J. D.; Mu, L.; Walsh, J.; Rahman, M. M.; Zydlewski, B.; Michel, F. M.; Xin, H. L.; Nordlund, D.; Lin, F. Accelerated Evolution of Surface Chemistry Determined by Temperature and Cycling History in Nickel-Rich Layered Cathode Materials. *ACS Appl. Mater. Interfaces* **2018**, *10* (28), 23842–23850.

(33) Nelson, J.; Yang, Y.; Misra, S.; Andrews, J. C.; Cui, Y.; Toney, M. F. Identifying and Managing Radiation Damage during in Situ Transmission X-Ray Microscopy of Li-Ion Batteries. *Proc. SPIE* **2013**, *8851*, 88510B.

(34) Bak, S. M.; Shadik, Z.; Lin, R.; Yu, X.; Yang, X. Q. In Situ/Operando Synchrotron-Based X-Ray Techniques for Lithium-Ion Battery Research. *NPG Asia Mater.* **2018**, *10*, 563–580.

(35) Borkiewicz, O. J.; Wiaderek, K. M.; Chupas, P. J.; Chapman, K. W. Best Practices for Operando Battery Experiments: Influences of X-Ray Experiment Design on Observed Electrochemical Reactivity. *J. Phys. Chem. Lett.* **2015**, *6* (11), 2081–2085.

(36) Borkiewicz, O. J.; Shyam, B.; Wiaderek, K. M.; Kurtz, C.; Chupas, P. J.; Chapman, K. W. The AMPIX Electrochemical Cell: A Versatile Apparatus for *in Situ* X-Ray Scattering and Spectroscopic Measurements. *J. Appl. Crystallogr.* **2012**, *45* (6), 1261–1269.

(37) Rahman, M. M.; Xu, Y.; Cheng, H.; Shi, Q.; Kou, R.; Mu, L.; Liu, Q.; Xia, S.; Xiao, X.; Sun, C.-J.; et al. Empowering Multi-component Cathode Materials for Sodium Ion Batteries by Exploring Three-Dimensional Compositional Heterogeneities. *Energy Environ. Sci.* **2018**, *11* (9), 2496–2508.

(38) Rahman, M. M.; Zhang, Y.; Xia, S.; Kan, W. H.; Avdeev, M.; Mu, L.; Sokaras, D.; Kroll, T.; Du, X.-W.; Nordlund, D.; et al. Surface Characterization of Li-Substituted Compositionally Heterogeneous NaLi_{0.045}Cu_{0.185}Fe_{0.265}Mn_{0.505}O₂ Sodium-Ion Cathode Material. *J. Phys. Chem. C* **2019**, *123* (18), 11428–11435.

(39) Gent, W. E.; Li, Y.; Ahn, S.; Lim, J.; Liu, Y.; Wise, A. M.; Gopal, C. B.; Mueller, D. N.; Davis, R.; Weker, J. N.; et al. Persistent State-of-Charge Heterogeneity in Relaxed, Partially Charged Li_{1-x}Ni_{1/3}Co_{1/3}Mn_{1/3}O₂ Secondary Particles. *Adv. Mater.* **2016**, *28* (31), 6631–6638.

(40) Wang, J.; Chen-Wiegart, Y. C. K.; Wang, J. In Operando Tracking Phase Transformation Evolution of Lithium Iron Phosphate with Hard X-Ray Microscopy. *Nat. Commun.* **2014**, *5* (1), 1–10.

(41) Yang, Y.; Xu, Z.; Steiner, J. D.; Liu, Y.; Lin, F.; Xiao, X. Quantitative Probing of the Fast Particle Motion during the Solidification of Battery Electrodes. *Appl. Phys. Lett.* **2020**, *116* (8), 081904.

(42) Mu, L.; Yuan, Q.; Tian, C.; Wei, C.; Zhang, K.; Liu, J.; Pianetta, P.; Doeff, M. M.; Liu, Y.; Lin, F. Propagation Topography of Redox Phase Transformations in Heterogeneous Layered Oxide Cathode Materials. *Nat. Commun.* **2018**, *9* (1), 2810.

(43) Hong, Y. S.; Huang, X.; Wei, C.; Wang, J.; Zhang, J. N.; Yan, H.; Chu, Y. S.; Pianetta, P.; Xiao, R.; Yu, X.; et al. Hierarchical Defect Engineering for LiCoO₂ through Low-Solubility Trace Element Doping. *Chem.* **2020**, *6* (10), 2759–2769.

(44) Zhang, S. S. Problems and Their Origins of Ni-Rich Layered Oxide Cathode Materials. *Energy Storage Mater.* **2020**, *24*, 247–254.

(45) Han, M.; Liu, Z.; Shen, X.; Yang, L.; Shen, X.; Zhang, Q.; Liu, X.; Wang, J.; Lin, H.; Chen, C.; et al. Stacking Faults Hinder Lithium Insertion in Li₂RuO₃. *Adv. Energy Mater.* **2020**, *10* (48), 2002631.

(46) Wang, D.; Kou, R.; Ren, Y.; Sun, C.-J.; Zhao, H.; Zhang, M.-J.; Li, Y.; Huq, A.; Ko, J. Y. P.; Pan, F.; et al. Synthetic Control of Kinetic Reaction Pathway and Cationic Ordering in High-Ni Layered Oxide Cathodes. *Adv. Mater.* **2017**, *29* (39), 1606715.

(47) Wang, R.; He, X.; He, L.; Wang, F.; Xiao, R.; Gu, L.; Li, H.; Chen, L. Atomic Structure of Li₂MnO₃ after Partial Delithiation and Re-Lithiation. *Adv. Energy Mater.* **2013**, *3* (10), 1358–1367.

(48) Mao, Y.; Wang, X.; Xia, S.; Zhang, K.; Wei, C.; Bak, S.; Shadik, Z.; Liu, X.; Yang, Y.; Xu, R.; et al. High-Voltage Charging-Induced Strain, Heterogeneity, and Micro-Cracks in Secondary Particles of a Nickel-Rich Layered Cathode Material. *Adv. Funct. Mater.* **2019**, *29* (18), 1900247.

(49) Romano Brandt, L.; Marie, J. J.; Moxham, T.; Förstermann, D. P.; Salvati, E.; Besnard, C.; Papadaki, C.; Wang, Z.; Bruce, P. G.; Korsunsky, A. M. Synchrotron X-Ray Quantitative Evaluation of Transient Deformation and Damage Phenomena in a Single Nickel-Rich Cathode Particle. *Energy Environ. Sci.* **2020**, *13* (10), 3556–3566.

(50) Xia, S.; Mu, L.; Xu, Z.; Wang, J.; Wei, C.; Liu, L.; Pianetta, P.; Zhao, K.; Yu, X.; Lin, F.; et al. Chemomechanical Interplay of Layered Cathode Materials Undergoing Fast Charging in Lithium Batteries. *Nano Energy* **2018**, *53*, 753–762.

(51) Wei, C.; Zhang, Y.; Lee, S. J.; Mu, L.; Liu, J.; Wang, C.; Yang, Y.; Doeff, M.; Pianetta, P.; Nordlund, D.; et al. Thermally Driven Mesoscale Chemomechanical Interplay in $\text{Li}_{0.5}\text{Ni}_{0.6}\text{Mn}_{0.2}\text{Co}_{0.2}\text{O}_2$ Cathode Materials. *J. Mater. Chem. A* **2018**, *6* (45), 23055–23061.

(52) Xu, R.; Yang, Y.; Yin, F.; Liu, P.; Cloetens, P.; Liu, Y.; Lin, F.; Zhao, K. Heterogeneous Damage in Li-Ion Batteries: Experimental Analysis and Theoretical Modeling. *J. Mech. Phys. Solids* **2019**, *129*, 160–183.

(53) Meirer, F.; Cabana, J.; Liu, Y.; Mehta, A.; Andrews, J. C.; Pianetta, P. Three-Dimensional Imaging of Chemical Phase Transformations at the Nanoscale with Full-Field Transmission X-Ray Microscopy. *J. Synchrotron Radiat.* **2011**, *18* (5), 773–781.

(54) Liu, Y.; Meirer, F.; Williams, P. A.; Wang, J.; Andrews, J. C.; Pianetta, P. TXM-Wizard: A Program for Advanced Data Collection and Evaluation in Full-Field Transmission X-Ray Microscopy. *J. Synchrotron Radiat.* **2012**, *19* (2), 281–287.

(55) Zhang, K.; Ren, F.; Wang, X.; Hu, E.; Xu, Y.; Yang, X. Q.; Li, H.; Chen, L.; Pianetta, P.; Mehta, A.; et al. Finding a Needle in the Haystack: Identification of Functionally Important Minority Phases in an Operating Battery. *Nano Lett.* **2017**, *17* (12), 7782–7788.

(56) Taiwo, O. O.; Finegan, D. P.; Gelb, J.; Holzner, C.; Brett, D. J. L.; Shearing, P. R. The Use of Contrast Enhancement Techniques in X-Ray Imaging of Lithium-Ion Battery Electrodes. *Chem. Eng. Sci.* **2016**, *154*, 27–33.

(57) Nazaretski, E.; Lauer, K.; Yan, H.; Bouet, N.; Zhou, J.; Conley, R.; Huang, X.; Xu, W.; Lu, M.; Gofron, K.; et al. Pushing the Limits: An Instrument for Hard X-Ray Imaging below 20nm. *J. Synchrotron Radiat.* **2015**, *22* (2), 336–341.

(58) Yan, H.; Bouet, N.; Zhou, J.; Huang, X.; Nazaretski, E.; Xu, W.; Cocco, A. P.; Chiu, W. K. S.; Brinkman, K. S.; Chu, Y. S. Multimodal Hard X-Ray Imaging with Resolution Approaching 10nm for Studies in Material Science. *Nano Futures* **2018**, *2*, 011001.

(59) Singer, A.; Sorgenfrei, F.; Mancuso, A. P.; Gerasimova, N.; Yefanov, O. M.; Gulden, J.; Gorniak, T.; Senkbeil, T.; Sakdinawat, A.; Liu, Y.; et al. Spatial and Temporal Coherence Properties of Single Free-Electron Laser Pulses. *Opt. Express* **2012**, *20* (16), 17480.

(60) Finegan, D. P.; Vamvakeros, A.; Tan, C.; Heenan, T. M. M.; Daemi, S. R.; Seitzman, N.; Di Michiel, M.; Jacques, S.; Beale, A. M.; Brett, D. J. L.; et al. Spatial Quantification of Dynamic Inter and Intra Particle Crystallographic Heterogeneities within Lithium Ion Electrodes. *Nat. Commun.* **2020**, *11*, 631.

(61) Jimenez-Sandoval, S. Micro-Raman Spectroscopy: A Powerful Technique for Materials Research. *Microelectron. J.* **2000**, *31* (6), 419–427.

(62) Pfeiffer, F. X-Ray Ptychography. *Nat. Photonics* **2018**, *12* (1), 9–17.

(63) Severson, K. A.; Attia, P. M.; Jin, N.; Perkins, N.; Jiang, B.; Yang, Z.; Chen, M. H.; Aykol, M.; Herring, P. K.; Fragedakis, D.; et al. Data-Driven Prediction of Battery Cycle Life before Capacity Degradation. *Nat. Energy* **2019**, *4* (5), 383–391.

(64) Kang, Y.; Li, L.; Li, B. Recent Progress on Discovery and Properties Prediction of Energy Materials: Simple Machine Learning Meets Complex Quantum Chemistry. *J. Energy Chem.* **2021**, *54*, 72–88.